Fabrication of W-doped VO_2 materials with low phase transition temperature for adaptive thermal camouflage application

Nguyen Duy Anh*, Nguyen Huu Van, Do Thi Thuy,
Nguyen Cong Thang, Khong Manh Hung

Institute of Materials, Biology and Environment/ Academy of Military Science and Technology, 17 Hoang Sam, Nghia Do, Hanoi, Vietnam.
*Corresponding author: nguyen.duy.anh0@gmail.com
Received 02 Oct. 2025; Revised 9 Dec. 2025; Accepted 10 Feb. 2026; Published 25 Feb. 2026.
DOI: https://doi.org/10.54939/1859-1043.j.mst.109.2026.63-69

ABSTRACT

This paper reports on the synthesis of W-doped VO_2 materials and the characterization of their phase transition temperature (PTT). Utilizing a microwave-assisted combustion synthesis method, the materials were successfully prepared with high homogeneity in particle size, while the processing time was shortened. The phase composition of the materials was determined by X-ray diffraction (XRD), which revealed that at certain doping levels, the material exhibited a structural change from monoclinic to tetragonal at room temperature. The morphology of the synthesized VO_2 was evaluated by scanning electron microscopy (SEM), showing uniform particle sizes of less than 200 nm. Differential Scanning Calorimetry (DSC) analysis indicated that the PTT of pure VO_2 was 67.2 °C. In contrast, as the W-doping concentration was incrementally increased (from 1% to 2%), the PTT decreased (from 44.4 °C down to 22.3 °C). The effective control of the phase transition temperature is crucial for the material's application in the field of adaptive thermal camouflage.

Keywords: Dynamic thermal camouflage; Combustion synthesis; W-doped VO_2.

1. INTRODUCTION

Infrared camouflage is a critical technique for thermal concealment, having garnered significant attention across a broad spectrum of commercial and military applications. Given that thermal imaging systems detect radiance patterns rather than kinetic temperature, thermal camouflage can be achieved through two primary mechanisms: the modulation of physical temperature or the manipulation of surface emissivity. In typical thermal camouflage scenarios, a high-temperature target must be concealed against a relatively cooler background. While direct active cooling is a feasible strategy, it is often suboptimal, as the dissipation of excess heat can result in detectable thermal emissions elsewhere in the system. Consequently, emissivity engineering presents a more practical and effective alternative to temperature regulation for achieving thermal stealth.

Vanadium dioxide (VO_2), which undergoes an insulator to metal transition around 68 °C, has been demonstrated as a metamaterial for emissivity engineering application [1], due to its ability to respond to environmental temperatures to modulate infrared irradiation from a transparent state at low-temperature to a reflective state at high-temperature [2]. Transiting from a low temperature monoclinic insulating phase to a high temperature rutile metallic phase, the infrared emissivity of VO2 changes significantly. But the practical application of pure VO_2 is limited by its high phase transition temperature; therefore, tungsten (W) doping is employed to effectively lower this threshold closer to room temperature. These promising properties make W-doped VO_2 an ideal key material in adaptive infrared camouflage.

The synthesis of phase pure thermochromic VO_2 presents significant challenges due to the multivalency of vanadium, which exhibits oxidation states ranging from 0 to +5. which usually correspond to a variety of binary oxides, such as V_2O_5, VO_2, V_2O_3, V_3O_7, and V_6O_{13}. Furthermore, the final crystalline structure is highly sensitive to fabrication parameters; depending on the synthesis method, VO_2 may crystallize into the rutile (R) or monoclinic (M1, M2) phases, as well

as several metastable polymorphs such as phases A, B, C, D, and T. [3]. Among these, the MIT only occurs reversibly between VO_2(M) and VO_2(R).

Several methodologies have been employed for the synthesis of vanadium oxide, including hydrothermal [4], sol-gel [5], chemical vapour deposition (CVD) [6], magnetron sputtering [7], spray pyrolysis [8], and so on. However, these methods have certain constraints, like the need for an inert-gas atmosphere, precise controlled flow, high temperature, a long synthesis period, and often require expensive and complicated equipment. In contrast, combustion synthesis (CS) offers an efficient way for producing the oxide, as it enables the rapid fabrication, which leads to the creation of relatively small-sized crystallites [9]. This process is further optimized by Microwave-Assisted Combustion Synthesis (MACS) by significantly reducing reaction times and promoting uniform heating of the precursor. This homogeneous heating minimizes temperature gradients, thereby suppressing the formation of secondary phases in the final product. Owing to these advantages, MACS has emerged as a preferred protocol for synthesizing oxides requiring high phase purity and controlled morphology.

2. EXPRIMENTAL

2.1. Materials

Ammonium metavanadate NH_4VO_3 99.95% (Macklin, China), ammonium paratungstate $(NH_4)_{10}H_2(W_2O_7)_6.4H_2O$ 99.95% (Macklin), glycine NH_2-CH_2-COOH 99% (Macklin), ammonium nitrate NH_4NO_3 99% (Duc Giang, Vietnam).

2.2. Experiment preparation

2.2.1. Monoclinic VO_2 synthesis

The synthesis of the VO_2 material was conducted via a microwave-assisted combustion synthesis technique. Conventionally, a combustion synthesis was conducted utilizing a nitrate salt that serves a dual function, acting as both the metal precursor and the primary oxidizer, in combination with a reducing agent that functions as the fuel source; however, owing to the unavailability of vanadium nitrate, an alternative precursor system was employed. The specific precursors selected were ammonium metavanadate NH_4VO_3 as the vanadium source, glycine as the fuel/reducing agent, and ammonium nitrate NH_4NO_3 as the oxidizer. The synthesis of VO_2 was performed according to the following equation:

$$NH_4VO_3 + 2\ C_2H_5NO_2 + 10\ NH_4NO_3 = VO_2 + 45/2\ N_2 + 4\ CO_2 + 27\ H_2O \quad (1)$$

In practice, carbon source may be oxidized to carbon monoxide CO along with carbon dioxide, and nitrogen products can range from ammonia NH_3 to nitrogen oxide NO_x, so the molar quantity of ammonium nitrate required for the reaction is expected to be lower than that predicted by the idealized stoichiometric equation (1). For the synthesis procedure, 10 mL of ammonium metavanadate (the vanadium source) 0.1 M was initially mixed with 10 mL glycine 0.2 M, in a fixed 1:2 molar proportion. The Fuel-to-Oxidizer ratio was systematically investigated across a range of 1:2 to 1:5. All precursor components were homogeneously mixed and subsequently introduced into a microwave oven. The reaction was executed until the combustion reaction was fully initiated (signaled by the emission of white smoke), at which point the heating was immediately terminated. The resulting solid product was then purified by multiple washing cycles utilizing deionized water and ethanol, followed by drying in an oven at 60 °C for 2 hours.

2.2.2. W-doped VO_2 synthesis

The synthesis of the W-doped VO_2 material was executed using the microwave-assisted combustion synthesis method previously optimized for pure VO_2. Initially, the tungsten precursor, $(NH_4)_{10}H_2(W_2O_7)_6.4H_2O$ was dissolved and then thoroughly mixed with the ammonium metavanadate solution for 30 minutes. The tungsten doping concentration was systematically

controlled in the range of 1% to 3% (molar ratio of W to V). Subsequently, the predetermined optimal molar ratio of fuel and oxidizer (established during the synthesis optimization of pure VO_2 were introduced). The remainder of the procedure was executed identically to the pure VO_2 synthesis protocol.

2.2.3. Characterization

The chemical phase of the as-synthesized products was determined using a PANalytical X-ray diffractometer (XRD). The product morphology and chemical composition were investigated using a Hitachi S-4800 field-emission scanning electron microscope (FE-SEM) equipped with an Energy-Dispersive X-ray Spectroscopy (EDX) detector. Finally, the thermotropic phase transition temperature was ascertained by Differential Scanning Calorimetry (DSC) using a NETZSCH DSC 204 F1 Phoenix system.

3. RESULTS AND DISCUSSION

3.1. X-ray diffraction study

The crystal structures of the synthesized vanadium oxide samples, prepared with various fuel to oxidant F/O ratios, were characterized using X-ray diffraction, with the results presented in figure 1. The XRD patterns collectively indicate a high degree of crystallinity, evidenced by the sharp and intense characteristic peaks exhibiting narrow bases. All un-doped samples display characteristic diffraction peaks at 2θ = 27.5°, 36.7°, 41.8°, 55.2°, 57.2°, 64.7°, and 70.2°. These peaks are successfully indexed to the (011), (200), (210), (220), (022), (013), and (-231) planes, respectively, of the monoclinic $P2_1/c$ VO_2 crystal structure (JCPDS No. 00-76-0456).

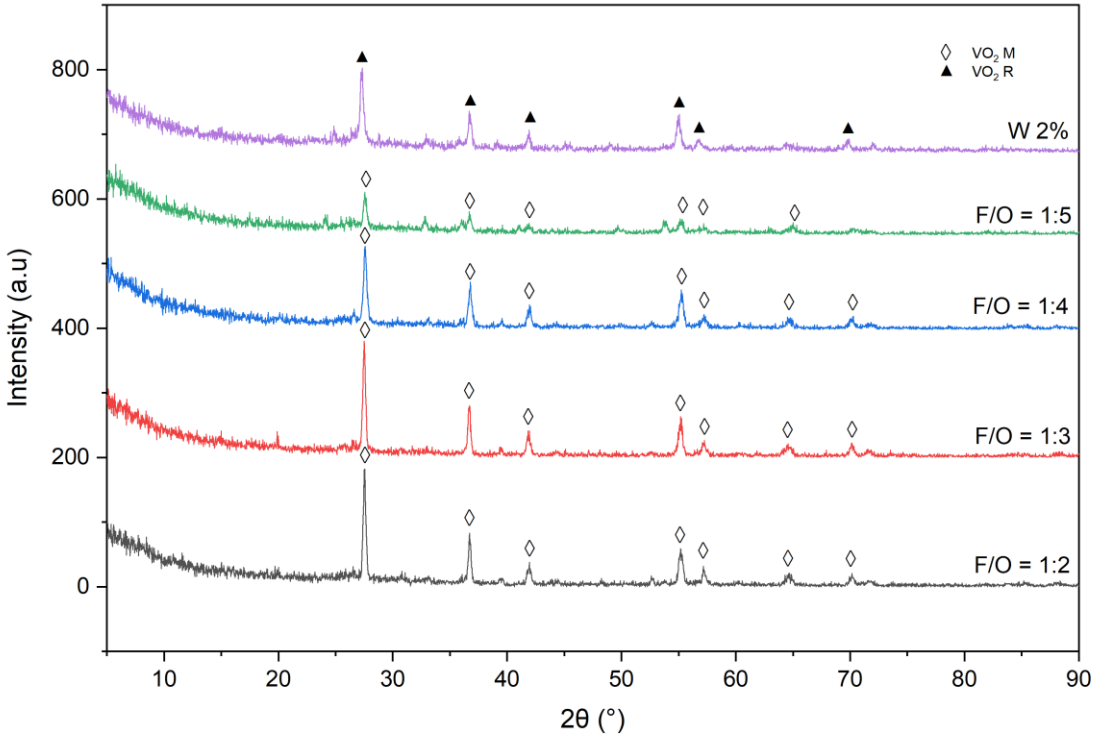

Figure 1. *X-ray diffraction pattern of synthesized VO_2.*

Among the un-doped products, the sample synthesized with an F/O ratio of 1:3 demonstrated the highest peak intensity, suggesting superior crystallinity. Experiments conducted at lower F/O

ratios showed a decrease in crystallinity, and the F/O = 1:2 experiment exhibited a slight decrease in product yield. Scherrer equation analysis on the (011) plane revealed an average crystallite size of 39.6 nm. Importantly, despite the variation in the oxidant-to-fuel ratio, no other vanadium oxides or VO_2 polymorphs were detected, indicated by the absence of extraneous peaks.

For the W-doped sample, the characteristic peaks shift to 2θ = 27.3°, 36.7°, 41.9°, 55.0°, 56.7°, and 69.8°. These peaks now correspond to the (110), (101), (111), (211), (220), and (301) planes of the rutile $P4_2/mnm$ VO_2 crystal lattice (JCPDS No. 01-076-0677). This result demonstrates that a 2%W-doping level effectively induces a crystal structure transformation from the monoclinic phase to the rutile phase at room temperature. It is noted that the characteristic peaks for the monoclinic and rutile forms are quite similar, highlighting the close structural relationship between the two phases, which explains the material's ability to undergo a reversible phase transition. Scherrer equation analysis applied to the (110) rutile plane indicates an average crystallite size of 27.7 nm, confirming that W-doping significantly reduces the crystallite size.

3.2. Chemical composition

The chemical composition of the synthesized W-doped vanadium oxide materials was quantitatively analyzed using Energy-Dispersive X-ray Spectroscopy (EDX). The primary objective of this analysis was to confirm the effective incorporation of the tungsten dopant and to verify the actual doping level against the nominal target concentrations.

The results at different locations and the average values, summarized in the table 1, demonstrate excellent congruence between the target nominal W molar ratios and the experimentally determined W atomic percentages.

Table 1. *Element composition and actual doping level of synthesized W-doped VO_2.*

Sample	Point 1		Point 2		Point 3		Average value		Actual W-doped level
	V	W	V	W	V	W	V	W	
1% W	39.35	0.41	40.38	0.41	46.62	0.5	42.12	0.44	1.03
2% W	34.75	0.69	34.67	0.65	30.37	0.76	33.3	0.7	2.06
3% W	33.43	1.11	33.77	1.22	34.22	1.2	33.8	1.18	3.36

For each targeted composition, the EDX analysis confirms successful doping, yielding measured average W concentrations of 1.03%, 2.06%, and 3.36%, respectively. The small, localized variation across the three measured points for each sample (Points 1, 2, and 3) validates the homogeneity of the dopant distribution within the synthesized powders.

This strong correlation between the nominal precursor stoichiometry and the measured final composition confirms the high efficiency and controllability of the microwave-assisted combustion synthesis method for precise W incorporation into the VO_2 lattice.

3.3. Morphology

The morphological structures of VO_2, and the doped one were examined using field-emission scanning electron microscopy (FE-SEM) (figure 2). The fabricated materials exhibit a particulate structure wherein primary particles are interconnected by small interparticle necks. This configuration yields a highly porous, space-filling network structure that is characteristic of materials synthesized via the rapid, gas-evolving nature of the combustion synthesis method.

A comparative analysis of the SEM micrographs reveals that the structure of the W-doped material is composed of significantly smaller primary particles and thinner connecting bridges compared to the un-doped sample. Compared to the undoped sample, the W-doped material exhibits a looser, more open microstructure.

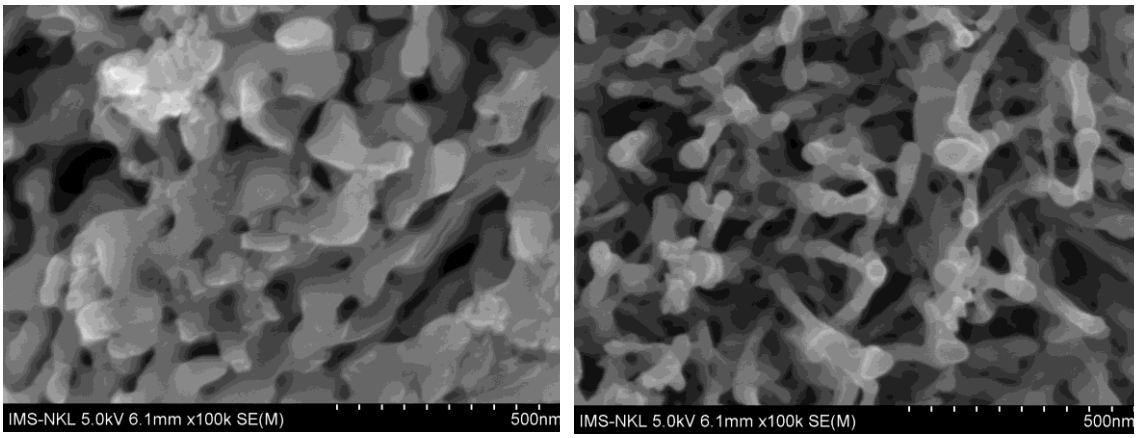

(a) *(b)*

Figure 2. *SEM images at 30.000 magnification of (a) undoped VO_2, (b) W-doped VO_2.*

This visual reduction in particle size, observed via SEM, is in excellent agreement with the decrease in crystallite size independently calculated from the Scherrer equation on the XRD data (39.6 nm for the un-doped sample versus 27.7 nm for the W-doped sample). This strong correlation is compelling evidence that the individual particles constituting the porous network are essentially single crystalline domains or composed of very few merged crystallites. Furthermore, the substantial reduction in particle size and increase in porosity confirm that the tungsten ion acts effectively as a crystal growth inhibitor during the high-temperature synthesis process.

3.4. Phase transition temperature

The DSC confirms that the phase transition temperature T_c of VO_2 M is highly sensitive to W-doping, exhibiting a clear, linear relationship between dopant concentration and the reduction of T_c. The experimental data for the Insulator-to-Metal Transition (IMT) temperature T_c is summarized below (table 2):

Table 2. *Phase transition temperature of undoped and W-doped VO_2.*

Samples	Phase transition temperature T_c (°C)	Calculated ΔT_c per 1%W (°C)
Undoped	67.2	-
1%W-doped	44.4	-22.8
2%W-doped	22.3	-22.1

The data reveal a striking and highly efficient suppression of the phase transition temperature. The T_c is reduced from the intrinsic value of 67.2 °C for the un-doped material to 44.4 °C at 1% W-doping and further down to 22.3 °C at 2% W-doping. This corresponds to an exceptionally high average reduction rate of approximately -22.5 °C per 1% atomic percent W incorporated.

The observed reduction is attributed to the substitution of the V^{4+} ion (r = 0.58 Å) with the larger, higher-valence W^{6+} ion (r = 0.60 Å) within the VO_2 lattice. This substitution introduces the extra two electrons donated by W^{6+} (replacing V^{4+}), partially fills the V 3d conduction band, thereby stabilizing the high-temperature metallic rutile phase and requiring less thermal energy to initiate the transition. The incorporation of the larger W^{6+} ion induces tensile strain in the lattice, which is the driving force for the IMT. This strain favors the metallic rutile phase, lowering the T_c. The high efficiency observed in this work (-22.5 °C/%W) is consistent with established literature, which consistently identifies tungsten as the most effective dopant for VO_2. [11]

4. CONCLUSIONS

In summary, we successfully utilized a microwave-assisted combustion synthesis route to prepare highly crystalline VO_2 nanoparticles, demonstrating high synthetic control by successfully optimizing the fuel/oxidant ratio to achieve the pure monoclinic phase. XRD analysis not only validated the phase purity but also confirmed a W-induced structural transformation to the rutile phase even at low doping concentrations. Elemental analysis by EDX confirmed the W-incorporation mechanism, showing excellent agreement between the nominal and measured doping levels. Furthermore, SEM characterization revealed a W-induced morphological evolution, confirming the undoped material's nanosized, porous network structure and demonstrating that the dopant successfully inhibited crystal growth, leading to a reduction in average crystallite size. Most critically, DSC analysis confirmed the high efficiency of the dopant, suppressing the phase transition temperature at a rate of (-22.5 °C per 1% W), highly consistent with literature, thereby positioning this material as a promising candidate for application in active thermal camouflage and next-generation thermochromic devices requiring operation near ambient temperature.

Acknowledgements: *The authors wish to express their sincere gratitude to the Institute of Environmental and Biological Materials for providing the necessary facilities and technical support that enabled the completion of this research.*

REFERENCES

[1]. H. Ji et al., *"Infrared thermochromic properties of monoclinic VO2 nanopowders using a malic acid-assisted hydrothermal method for adaptive camouflage"*, RSC Adv., Vol. 7, pp. 5189–5194, (2017).

[2]. M.E.A. Warwick and R. Binions, *"Advances in thermochromic vanadium dioxide films"*, J. Mater. Chem. A, Vol. 2, pp. 3275–3292, (2014).

[3]. Wen C et al., *"A review of the preparation, properties and applications of VO2 thin films with the reversible phase transition"*, Front. Mater., Vol. 11, art. no. 1341518, (2024).

[4]. H.T. Zhang et al., *"Imprinting of local metallic states into VO2 with ultraviolet light"*, Adv. Funct. Mater., Vol. 26, pp. 6612–6618, (2016).

[5]. D. Ruzmetov, K.T. Zawilski, V. Narayanamurti, and S. Ramanathan, *"Structure-functional property relationships in rf-sputtered vanadium dioxide thin films"*, J. Appl. Phys., Vol. 102, art. no. 113715, (2007).

[6]. M.E.A. Warwick, I. Ridley, and R. Binions, *"Thermochromic vanadium dioxide thin films from electric field assisted aerosol assisted chemical vapour deposition"*, Sol. Energy Mater. Sol. C, Vol. 143, pp. 592–600, (2015).

[7]. L. Mathevula et al., *"Thermochromic VO2 on zinnwaldite mica by pulsed laser deposition"*, Appl. Surf. Sci., Vol. 314, pp. 476–480, (2014).

[8]. M.M. Seyfouri and R. Binions, *"Sol-gel approaches to thermochromic vanadium dioxide coating for smart glazing application"*, Sol. Energy Mater. Sol. C, Vol. 159, pp. 52–65, (2017).

[9]. Delaram Mahmoudi, Mansour Soltanieh, and Hossein Aghajani, *"Low-cost solution combustion synthesis of monoclinic VO2(M) for thermochromic smart windows: Optimization, characterization, and simulation"*, Journal of Alloys and Compounds, Vol. 1037, art. no. 182199, (2025).

[10]. H. Wu et al., *"Direct synthesis of vanadium oxide nanopowders by the combustion approach"*, Chemical Physics Letters, Vol. 706, pp. 7–13, (2018).

[11]. N. Wang et al., *"Single-Crystalline W-Doped VO2 Nanobeams with Highly Reversible Electrical and Plasmonic Responses Near Room Temperature"*, Advanced Materials Interfaces, Vol. 3, no. 16, pp. 160-164, (2016).

TÓM TẮT

Chế tạo vật liệu VO_2 pha tạp W có nhiệt độ chuyển pha thấp định hướng ứng dụng trong ngụy trang nhiệt chủ động

Nghiên cứu này trình bày quá trình tổng hợp và đánh giá nhiệt độ chuyển pha của vật liệu VO_2 pha tạp bằng W. Sử dụng phương pháp tổng hợp đốt cháy kết hợp với sự hỗ trợ của vi sóng, vật liệu được chế tạo thành công với độ đồng đều cao về kích thước hạt, trong khi thời gian tiến hành được rút ngắn. Thành phần pha của vật liệu được xác định bằng phương pháp nhiễu xạ tia X (XRD), cho thấy với mức độ pha tạp nhất định, vật liệu có sự thay đổi cấu trúc từ đơn nghiêng sang tứ phương (ở nhiệt độ thường). Hình thái học của VO_2 chế tạo được được đánh giá bằng phương pháp hiển vi điện tử quét SEM, cho thấy kích thước hạt đồng nhất và nhỏ hơn 200 nm. Kết quả phân tích nhiệt vi sai của vật liệu cho thấy nhiệt độ chuyển pha của vật liệu VO_2 tinh khiết là 67.2 °C, trong khi đó, việc bổ sung lượng pha tạp của W tăng dần (từ 1% lên 2%) làm nhiệt độ chuyển pha giảm (từ 44.2 °C xuống 22.3 °C). Việc kiểm soát tốt nhiệt độ chuyển pha là mấu chốt để đưa vật liệu vào ứng dụng trong lĩnh vực ngụy trang ảnh nhiệt chủ động.

Từ khoá: Ngụy trang ảnh nhiệt chủ động; Tổng hợp đốt cháy; VO_2 pha tạp W.